

Effect of thickness on optoelectrical properties of Nb-doped indium tin oxide thin films deposited by RF magnetron sputtering

LI Shi-na (李士娜), MA Rui-xin (马瑞新)*, MA Chun-hong (马春红), LI Dong-ran (李东冉), XIAO Yu-qin (肖玉琴), HE Liang-wei (贺良伟), and ZHU Hong-min (朱鸿民)

Department of Non-ferrous Metallurgy, School of Metallurgical and Ecological Engineering, University of Science and Technology Beijing, Beijing 100083, China

(Received 11 January 2013)

©Tianjin University of Technology and Springer-Verlag Berlin Heidelberg 2013

Niobium-doped indium tin oxide (ITO:Nb) thin films are prepared on glass substrates with various film thicknesses by radio frequency (RF) magnetron sputtering from one piece of ceramic target material. The effects of thickness (60–360 nm) on the structural, electrical and optical properties of ITO: Nb films are investigated by means of X-ray diffraction (XRD), ultraviolet (UV)-visible spectroscopy, and electrical measurements. XRD patterns show the highly oriented (400) direction. The lowest resistivity of the films without any heat treatment is $3.1 \times 10^{-4} \Omega \cdot \text{cm}^{-1}$, and the resistivity decreases with the increase of substrate temperature. The highest Hall mobility and carrier concentration are 17.6 N·S and $1.36 \times 10^{21} \text{ cm}^{-3}$, respectively. Band gap energy of the films depends on substrate temperature, which varies from 3.48 eV to 3.62 eV.

Document code: A **Article ID:** 1673-1905(2013)03-0198-3

DOI 10.1007/s11801-013-2411-1

Transparent and conductive oxide (TCO) thin films have been widely used as transparent electrode for flat panel displays and photovoltaic technologies^[1,2]. More recently, TCO films have been used for flat panel displays including liquid crystal displays (LCDs), organic light emitting diodes and plasma displays. Among the various TCO thin films, tin doped indium oxide (ITO) films are widely used in flat displays, solar cells, architectural glasses and other fields^[3]. ITO film is a heavily doped, high-degenerate n-type semiconductor with a good electrical conductivity and transmittance in visible region. It also has the resistance to chemical corrosion and the good processing performance^[4]. ITO films can be prepared by variety of techniques, such as magnetron sputtering^[5], ion assisted deposition^[6], pulsed laser deposition (PLD)^[7], dip coating^[8], ion beam sputtering^[9], sol-gel^[10], and reactive thermal evaporation^[11]. Magnetron sputtering not only offers the possibility of preparing ITO films at low processing temperature and on large areas^[12], but also obtains excellent optical and electrical properties. So it is widely used in thin film technology.

With the continuous development of thin film technology, dual-ITO thin film is unable to meet higher performance requirements. The photoelectrical properties of traditional binary ITO ($\text{In}_2\text{O}_3:\text{SnO}_2$) films can be improved by doping other elements. Besides tin (Sn), other elements, such as zirconium (Zr)^[13], tantalum (Ta)^[14], titanium (Ti)^[15], molybdenum (Mo)^[16], tungsten (W)^[17],

cerium (Ce)^[18] and silver (Ag)^[19], have also been employed as dopants. Among these researches, MoO_3 , WO_3 and Ta are too easy to sublime and difficult to be doped into In_2O_3 crystal structure. Ti and Zr have the same ionic valance with tin. S. M. Chung et al^[20] have investigated the effect of titanium doping on the structural, optical and electrical properties of ITO: Ti films by direct current (DC) co-sputtering of metallic titanium and ceramic ITO target materials. The results show that the lowest resistivity is $2.3 \times 10^{-4} \Omega \cdot \text{cm}^{-1}$, and the carrier concentration is $6.24 \times 10^{20} \text{ cm}^{-3}$ after heat treatment. It is still challenge to reduce the electrical resistivity and maintain the transmittance in visible range simultaneously.

In this paper, we demonstrate that by controlling the cationic composition in ITO-based oxide films deposited by radio frequency (RF) magnetron sputtering using only one piece of niobium-doped ITO (ITO:Nb) ceramic target material, the properties of the ITO:Nb films can be optimized. The structural, electrical and optical properties of Nb-doped ITO (ITO:Nb) films at different substrate temperatures are investigated.

The sputtering target material was made of ITO powder (99.99%) mixed with Nb_2O_5 powder (99.99%) through blending, moulding and sintering processes. The composition of In: Sn: Nb: O in ITO:Nb target is 66.31%: 7.59%: 0.77%: 20.4 %.

Corning Eagle 2000 (20 mm×20 mm×0.7 mm) glass, for thin film transistor (TFT)-LCD, was used as substrate

* E-mail: maruixin@ustb.edu.cn

to prepare ITO:Nb thin films by RF magnetron sputtering from as-prepared ITO:Nb ceramic target materials at RF power of 40 W. The sputtering was carried out at room temperature. The target-substrate distance was 60 mm, and the base pressure in the sputtering chamber was 2×10^{-4} Pa. High pure argon gas ($10 \text{ cm}^3/\text{min}$, 99.999%) was introduced into sputtering chamber to maintain a working pressure of 0.80 Pa. All glass substrates were ultrasonically cleaned in acetone, ethanol and de-ionized water in turn, and then dried before sputtering.

The structural characteristics and morphology were performed by X-ray diffraction (XRD) and atomic force microscopy (AFM). The XRD spectra of all the films were recorded with Rigaku D/max-RB X-ray diffractometer (Rigaku, Tokyo, Japan, 40 kV, 150 mA) using Cu K α radiation ($\lambda=0.15406 \text{ nm}$). The AFM image was performed under ambient conditions using a Digital Instruments (Veeco) Dimension-3100 unit with Nanoscope1 III controller, operating in tapping mode. The transmittance curves of the bare and the ITO:Nb coated glass substrates were measured in the wavelength range of 300–800 nm by a spectrophotometer. Electrical resistivity, Hall mobility and carrier concentration of the ITO:Nb films were measured using the Van de Pauw method.

Typical XRD patterns of the as-prepared ITO:Nb thin films grown with different film thicknesses are shown in Fig.1. All the films are highly oriented (400) direction, and the peak position is consistent with the JCPDS file card No.6-0416 for In_2O_3 , which is in agreement with the previous works^[21,22]. It illustrates that doping with niobium and tin can not result in the development of new crystal orientations or the changes of preferential orientations, which indicates that all samples consist of In_2O_3 phase, despite of the presence of niobium and tin dopant. This result implies that niobium and tin, added into the target materials, can not change the phase structure of In_2O_3 films, and have been doped into the crystal structure of In_2O_3 .

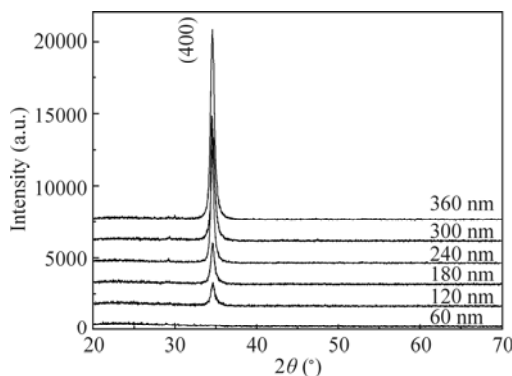


Fig.1 XRD patterns of ITO:Nb films with different thicknesses

The carrier concentration and Hall mobility of ITO:Nb thin films with different thicknesses are shown in Fig.2. The electrical resistivity of ITO:Nb film is determined by the resistance and thickness of film. It is observed that the resistivity of the films increases and then decreases

with the increase of thickness. The minimum resistivity is $3.1 \times 10^{-4} \Omega \cdot \text{cm}$ with the thickness of 180 nm. Conversely, it is observed that the Hall mobility of the films decreases and then increases with the increase of thickness. On the other hand, the carrier concentration is found to increase with the increase of film thickness. The maximum Hall mobility and carrier concentration are 17.6 N·S and $1.36 \times 10^{21} \text{ cm}^{-3}$, respectively. The above phenomenon may be explained on the basis of film crystallinity. The decrease of resistivity in ITO:Nb films with the increase of thickness is ascribed to the gradual decrease of the substrate film. With the decrease of the substrate film, the crystallization and grain size lead to the reduction of grain boundary scattering, lattice defects, electron trap and the decrease of electrical resistivity^[23]. But superabundant accumulating of the adsorbed oxygen atoms on the grain boundaries makes the carrier concentration decrease, leading to the decrease of the Hall mobility after the film thickness more than 180 nm. Thus, it makes the resistivity increase.

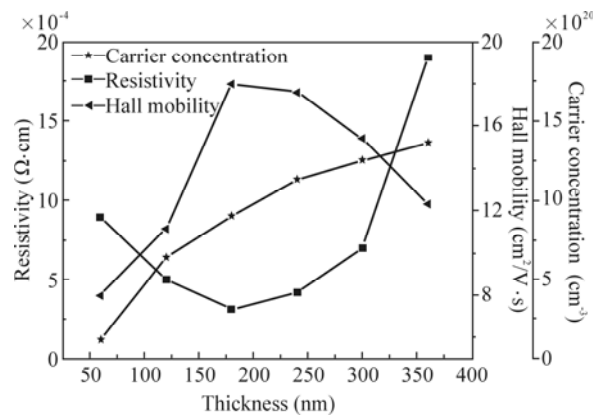


Fig.2 Electrical properties of ITO:Nb films with different film thicknesses

Fig.3 shows the optical transmittance curves of ITO:Nb films with different thicknesses. The average transmittance is greater than 87%. It is also observed from Fig.3 that films exhibit red shift of the absorption edge to short wavelength in the UV region due to size effect. Fig.4

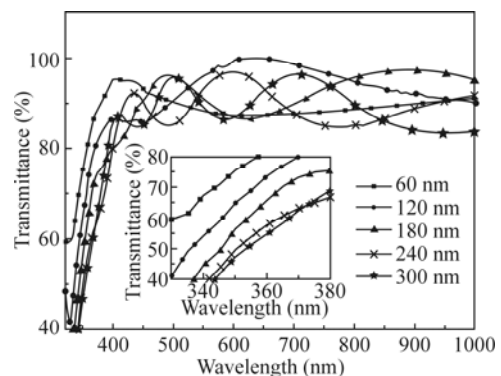


Fig.3 Transmittance curves of ITO:Nb films with different thicknesses

shows the relationship between $(\alpha hv)^2$ and hv for ITO:Nb films with different thicknesses. It is found that the band gap is increased with the increase of thickness. The maximum band gap of ITO:Nb film is 3.62 eV at 300 nm. The calculated band gaps of ITO:Nb films at various film thicknesses are listed in Tab.1.

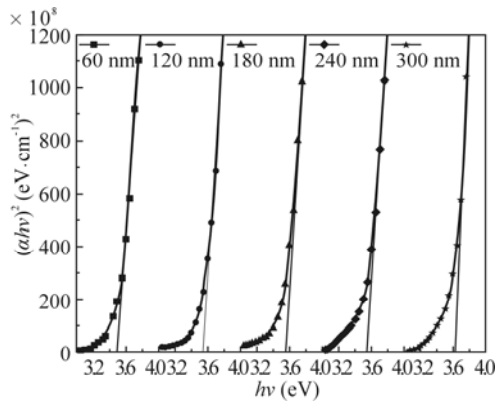


Fig.4 $(\alpha hv)^2$ vs. hv in ITO:Nb films with different film thicknesses

Tab.1 Band gaps of ITO:Nb films with different film thicknesses

Thickness (nm)	60	120	180	240	300
Band gap (eV)	3.48	3.57	3.57	3.58	3.62

ITO:Nb thin films are fabricated on glass substrates by RF magnetron sputtering with various thicknesses from ceramic target materials. Structural, electrical and optical properties of the films are investigated by using XRD, UV-visible spectroscopy and electrical measurements. The XRD patterns show a polycrystalline structure of ITO:Nb films similar to pure In_2O_3 phase. The optimized ITO:Nb film exhibits the lowest resistivity of $3.1 \times 10^{-4} \Omega \cdot cm$. The highest Hall mobility and carrier concentration are $17.6 N \cdot S$ and $1.36 \times 10^{21} cm^{-3}$, respectively. All films have an average transmittance of above 87%, indicating that such ITO:Nb films can be applied for various optical and electronic devices.

References

[1] D. S. Ginley et al, Handbook of Transparent Conductors, 1 (2010).
 [2] A. E. Delahoy, L. Chen, M. Akhtar, B. Sang and S. Guo, Solar Energy **77**, 785 (2004).

[3] R. B. H. Tahar, T. Ban, Y. Ohya and Y. Takahashi, J. Appl. Phys. **83**, 2631 (1998).
 [4] E. Aperathitis, M. Bender, V. Cimalla, G. Ecke and M. Modreanu, J. Appl. Phys. **94**, 1258 (2003).
 [5] Y. F. Lan, W. C. Peng, Y. H. Lo and J. L. He, Materials Research Bulletin **44**, 1760 (2009).
 [6] L. J. Meng, J. Gao, M. P. dos Santos, X. Wang and T. T. Wang, Thin Solid Films **516**, 1365 (2008).
 [7] J. P. Zheng and H. S. Kwok, Applied Physics Letters **63**, 1 (1993).
 [8] F. L. Akkad, A. Punnose and J. Prabu, J. Appl. Phys. A **71**, 157 (2000).
 [9] T. Sasabayashia, N. Itoa, E. Nishimuraa, M. Kona, P. K. Songa, K. Utsumib, A. Kaijoc and Y. Shigesato, Thin Solid Films **445**, 219 (2003).
 [10] A. Luis, C. Nunes de Carvalho, G. Lavareda, A. Amaral, P. Brogueira and M. H. Godinh, Vacuum **64**, 475 (2002).
 [11] G. S. Belo, B. J. P. da Silva, E. A. de Vasconcelos, W. M. de Azevedo and E. F. da Silva Jr, Applied Surface Science **255**, 755 (2008).
 [12] A. Amaral, P. Brogueira, C. Nunes de Carvalho and G. Lavareda, Journal of Nanoscience and Nanotechnology **10**, 2713 (2010).
 [13] B. Zhang, X. F. Xu, X. P. Dong and J. S. Wu, Optoelectronics Letters **4**, 137 (2008).
 [14] B. Zhang, B. Yu, X. F. Xu and P. Zhao, Journal of Optoelectronics · Laser **21**, 59 (2010). (in Chinese)
 [15] B. Zhang, X. P. Dong, X. F. Xu, X. J. Wang and J. S. Wu, Materials Science in Semiconductor Processing **10**, 264 (2007).
 [16] S. H. Paeng, M.W. Park and Y. M. Sung, Surface and Coatings Technology **205**, 210 (2010).
 [17] R. K. Gupta, K. Ghosh, R. Patel and P.K. Kahol, Applied Surface Science **518**, 3081 (2010).
 [18] M. Yang, J. H. Feng, G. F. Li and Q. Zhang, Journal of Crystal Growth **310**, 3474 (2008).
 [19] Y. M. Kang, S. H. Kwon, J. H. Choi, Y. J. Cho and P. K. Song, Surface and Coatings Technology **205**, 210 (2010).
 [20] C. B. Cao, A. Y. Zhou, S. H. Mu, G. S. Zhang, X. P. Song and Z. Q. Sun, Materials Science and Engineering: B **176**, 1430 (2011).
 [21] S. M. Chung, J. H. Shin, W. S. Cheong, C. S. Hwang, K. I. Choa and Y. J. Kim, Ceramics International **38**, s617 (2012).
 [22] S. N. Li, R. X. Ma, C. H. Ma, L. W. He, Y. Q. Xiao, J. G. Hou and S. Q. Jiao, Optoelectronics Letters **8**, 460 (2012).
 [23] N. Zhang, J. X. Liu and S. N. Zeng, Rare Metal Materials and Engineering **37**, 164 (2008).